Journal of Metals, Materials and Minerals, 34(1), 1787, 2024

A contribution to the exploration of the chemical durability, thermal stability, and structural ability of glasses from the Fe_2O_3-K_2O-MoO_3-P_2O_5 quaternary system

Asmae ER-RAFAI[1], Yasmina ALAOUI[1], Mohamed LAOURAYED[1], Mohamed OUNACER[2], Mouloud EL MOUDANE[1,*], Mohammed SAJIEDDINE[2], and Abdelkbir BELLAOUCHOU[1]

[1] *Laboratory of Materials, Nanotechnology, and Environment, Faculty of Science, Mohammed V University in Rabat, P.O. Box. 1014, Agdal-Rabat, Morocco*

[2] *Physic of Materials Laboratory, FST, Sultan Moulay Slimane University, Beni-Mellal, Morocco*

***Corresponding author e-mail:** m.elmoudane@gmail.com

Received date:
9 July 2023
Revised date
7 December 2023
Accepted date:
30 December 2023

Keywords:
Phosphate glasses;
Iron oxide;
IR et Raman;
Mössbauer spectroscopy;
Chemical durability

Abstract

The relationships between the properties and structure of xFe_2O_3-$(40-x)K_2O$-$10MoO_3$-$50P_2O_5$ glasses have been reported in this paper. Homogeneous glasses are formed for different Fe_2O_3 contents. The density and molar volume evolution of these glasses shows that Fe_2O_3 acts as a glass former and strengthens the structural bonds of the glass. Experimental ^{57}Fe Mössbauer spectroscopy graphs suggest the existence of divalent Iron (Fe^{II}) and trivalent Iron (Fe^{III}). The boost in chemical durability agrees with the growth in glass transition temperature due to more powerful bonding in the structural network. P-O-Fe bonds replace P-O-P bonds when Fe_2O_3 is present in the phosphate network.

1. Introduction

All materials can undergo environmental degradation; the rate and degree of degradation depend on the details of the material's composition, structure, and environment [1]. Phosphate glass materials represent a great interest in technological fields. They are widely studied in research [2-13]. However, their relatively poor chemical durability limits their use. In alkali metal oxides such as K_2O, the three-dimensional networks are converted into linear phosphate chains, resulting in the breakage of the P-O-P bond and the generation of non-bridging oxygens [14]. Transition metal ion-containing glasses, particularly Fe_2O_3 and MoO_3, have attracted considerable interest given their potential use in electrochemical, electronic, and electro-optical devices [15-17]. As such, phosphate glasses containing Iron are now being researched for various technical purposes because of their exceptional chemical durability, relatively lower melting temperature, and elevated waste-loading capacity [18-24].

On the other hand, Fe^{2+} and Fe^{3+} assumed to play additional structural functions in phosphate glasses incorporating iron oxide, affect the structure [25]. According to the IR data, iron ions act as network formers and modifiers relying upon the Fe^{2+}/Fe^{3+} ratio [19,26]. In addition, the presence of Fe_2O_3 in the phosphate network causes the P=O to break, and the P-O-P bonds are replaced by P-O-Fe bonds.

Many studies have found that the effect of iron oxide on structural, thermal, and chemical durability relies on the glass material's composition. The influence of Fe_2O_3 composition on the chemical durability of phosphate glass comprising Zinc, especially on the glass series $(40-x)ZnO$-xFe_2O_3-$60P_2O_5$ (x=10 mol% to 40 mol%), shows that the durability increases considerably with the rising of Fe_2O_3 percentage [27]. From the infrared spectra, Moustafa *et al.* [19] discovered that adding Fe_2O_3 significantly affects the local order of the glass network of glassy phosphate. Ma *et al.* [28] demonstrated that substituting sodium for iron results in a broader phosphate anions distribution in glasses due to disproportionation reactions. The consistent shifts in Raman frequencies imply no preferred iron replacement with sodium at a specific phosphate site. EPR data indicate that Fe^{3+} ions are not restricted to the center positions of the glass formers' tetrahedral and octahedral sites but can also be located at interstitial or peripheral points in the glass matrix [29]. Thus, it is proven that sodium-free iron phosphate glasses' thermal stability versus crystallization is often higher than sodium-containing iron phosphate glasses [30]. Beloued *et al.* [31] explained that increased Fe_2O_3 in the glass composition results in stronger bonds in the glassy system. Incorporating Fe^{2+} and Fe^{3+} strengthens the Fe-O-P covalent bond and increases the rigidity of the glass. The generation of short pyrophosphate chains, as indicated by the IR and XRD spectra, gives significant chemical durability.

In addition, Mössbauer spectroscopy has been used to study a wide range of phenomena in materials science, solid-state physics, and chemistry. It can provide detailed information about the electronic

and magnetic properties of materials, as well as the local atomic environment, lattice dynamics, and phase transitions. It is particularly useful for studying the behavior of certain isotopes, such as iron, which are common in many materials.

Mössbauer spectroscopy can be combined with other experimental techniques, such as X-ray diffraction, Infrared spectroscopy, Raman spectroscopy, and other characterization methods, to obtain a more complete and detailed view of the properties of the materials studied.

Motivated by the above consideration, this article aims to explore the Structure-property and chemical durability relationships of a new glass of general composition xFe_2O_3-(40-x)K_2O-10MoO_3-50P_2O_5 with (x=10, 20, 30, 40). The anticipated results of our study will yield valuable insights for the examination and implementation of high-level nuclear waste disposal. Specifically, we aim to resolve the issue of diminished chemical durability in phosphate glasses. In addition, the phosphate glasses were studied by X-ray diffraction (XRD), Differential scanning calorimetry (DSC), Fourier transforms infrared (FT-IR), and Raman spectroscopy to examine alterations in the glass structure as a result of the content. In parallel, we examined the iron sites within the glass using ^{57}Fe Mössbauer spectroscopy. Combining this with an assessment of the glass's chemical durability, we were able to determine the role of iron in the dissolution process. To test the glass's chemical durability, three different solutions were used: HCl solution, deionized water, and NaOH solution.

2. Materials and methods

2.1 Glass preparation

A molybdenum phosphate derivatives glass containing various percentages of potassium and iron oxide was carried out. This study used all commercial chemical reagents, $NH_4H_2PO_4$, $(NH_4)_6Mo_7O_{24}$, $4H_2O$, K_2CO_3, and Fe_2O_3, which are of high-purity reagent grade (99%, Sigma-Aldrich) with precise proportions for each composition. Glasses of composition xFe_2O_3-(40-x) K_2O-10MoO_3-50P_2O_5 with (x=10, 20, 30, 40) were elaborated via the traditional melt-quenching technique [32,33]. All batches were loaded into an alumina crucible and underwent a two-hour heat treatment, with temperatures varying between 200°C and 500°C. The purpose of this step was to remove residual ammonia, water, and carbon dioxide. Subsequently, the temperature was gradually increased to 1100°C and maintained at this level for half an hour. The resulting melt was quickly quenched under ambient air conditions, resulting in the production of vitreous samples. The compositions investigated in the present study are summarized in Table 1.

2.2 Glass characterization

X-ray diffraction (XRD) patterns of the amorphous state of the glass system were recorded using an X-ray powder diffractometer. The XRD graphs were created at an ambient temperature using a Siemens D5000 powder diffractometer with a CuK_α radiation source ($\lambda_{CuK\alpha}$= 0. 5418 Å) at a scanning speed of 2° per minute in 2θ, from 10° to 60°.

Density measurements were performed at room temperature via the Archimedes method with diethyl phthalate as the immersion fluid. The uncertainty of the density measurements was approximately ± 0.005 $g{\cdot}cm^{-3}$.

Differential scanning calorimetry (DSC-SETRAM) determines the glass transition temperatures at a heating rate of 10°C·min^{-1} in an argon atmosphere with an uncertainty of ± 5°C.

The different samples' FT-IR spectra were measured on Bruker Platinum-ATR apparatus type functioning in transmittance mode at room temperature between 400 cm^{-1} and 1400 cm^{-1}.

The Raman spectra are carried out on a Renishaw micro-Raman spectrometer RM1000 coupled to a He-Ne laser 19 mW for wave numbers 100 cm^{-1} to 1100 cm^{-1} via the 632.8 nm line at room temperature.

The coordination environment of polyhedral Iron (FeO_n) and its valence states in the glassy matrix was analyzed using a Mössbauer spectrometer (Wissel GmbH) standard transmission configuration ^{57}Fe at room temperature. The hyperfine spectral parameters were calculated using the NORMOS least squares fitting program.

2.3 Chemical durability

The chemical durability of a glass is a measure of its resistance to attack by chemical agents. The physical forms which the glass may take, and the nature and conditions of the chemical attack are many and various. This means that there is no one standard measure of durability and glasses are instead classified relative to one another after subjection to the same experimental conditions. Various methods are used to assess the results of durability experiments. The weight loss measurement is carefully selected.

Because of evaluating the chemical durability of iron oxide doped glasses, durability experiments were performed. Glass samples were first immersed in deionized water, acidic medium HCl, and alkaline solution NaOH at ambient temperature at fixed time intervals, then removed from the solution, rinsed, dried, weighed and returned to the solution.

The weight loss (W) of the specimen at different times (t) was used to calculate the dissolution rate (DR) of these glasses:

$$DR = \Delta W/(A \times t) \quad (1)$$

Where: ΔW is the weight loss (g), A is the surface area (cm^2), and t is the immersion time (min).

Table 1. Physical parameters: Density ρ ($g.cm^{-3}$), molar volume V_M ($cm^3.mol^{-1}$) and glass transition temperature T_g (°C) of xFe_2O_3-(40-x)K_2O-10MoO_3-50P_2O_5 glasses.

X	xFe_2O_3-(40-x)K_2O-10MoO_3-50P_2O_5						
	Composition (mol %)				ρ	V_M	T_g
	Fe_2O_3	K_2O	MoO_3	P_2O_5	($g.cm^{-3}$)	($cm^3.mol^{-1}$)	(°C)
0	0	40	10	50	2.96	41.50	429
10	10	30	10	50	3.08	44.41	451
20	20	20	10	50	3.14	47.99	457
30	30	10	10	50	3.36	48.88	477

3. Results and discussion

3.1 X-ray diffraction

X-ray diffraction (XRD) spectra of all compositions are presented in Figure 1. In this study, the X-ray diffraction results were presented in their raw data form without further processing or normalization. The unprocessed data allows for a more direct examination of the amorphous nature of all the synthesized glassy compositions. There is a wide scattering ranging between $2\theta = 15°$ to 30°. The uniform absence of sharp diffraction peaks across all samples indicates their homogenous amorphous nature, confirming the successful synthesis of glassy materials.

3.2 Physical properties

Density is a physical parameter sensitive to atoms' spatial arrangement in the glassy lattice. Various parameters determine it, including the interstitial space's structure, molecular weight, coordination number, and dimensionality [34]..

Figure 2 illustrates both ρ and V_m dependence of the composition of Fe_2O_3 in xFe_2O_3-(40-x) K_2O-10MoO_3-50P_2O_5 glasses. Following the results (Figure 2 and Table 1), the increase in molar volume as the density of a material increases can be understood through fundamental principles in materials science. To clarify this relationship, it's essential to delve into the definitions of density and molar volume, as well as the effects of different chemical components on the glass structure.

Density, defined as mass per unit volume, is expressed mathematically as $\rho = M/V$, where ρ is density, M is molar mass, and V is molar volume. Conversely, molar volume can be determined using the formula $V = M/\rho$.

In our study, the measured density increased when K_2O was substituted with Fe_2O_3. This is due to the notably higher molar mass of iron compared to potassium ($M_K = 39.0983$ g·mol^{-1} < $M_{Fe} = 55.854$ g·mol^{-1}). As a result, the overall molar mass of the glass composition increased as Fe_2O_3 content rose, which, in turn, affected the molar volume. In the molar volume formula, both molar mass and density are influenced by the introduction of Fe_2O_3, providing a coherent explanation for the observed increase in molar volume with rising Fe_2O_3 concentration.

Furthermore, it's crucial to consider the potential alterations in the coordination environment of Fe^{3+} ions within the glass structure compared to K^+ ions. Changes in coordination can significantly impact the arrangement of atoms and interatomic distances, which may contribute to an expansion in volume. This alteration in the coordination environment and its effects on the glass structure should not be overlooked. Thus, the addition of Fe_2O_3 inside the glassy network, leads to a potential expansion of the present amorphous matrix. Thus, this behavior occurs when Fe_2O_3 acts as a glass former and strengthens the structural bonds of the glass [35].

3.3 Thermal studies

DSC curves in Figure 3 and the corresponding data in Table 1 vividly illustrate the profound impact of Fe_2O_3 content on the thermochemical properties of phosphate glass. It's noteworthy that as the Fe_2O_3 content increases, the glass transition temperature (T_g) experiences a substantial rise, as evident in Figure 4. This phenomenon is intricately linked to the rigidity of the glass matrix [31], as an increase in T_g implies a more stable and structurally ordered glass. The correlation between T_g and the chemical composition of the glass is well-established in the literature, where an increase in oxidation degree or coordination often leads to higher T_g values. Additionally, variations in ionic radius can influence T_g, with smaller ionic radii contributing to increased T_g. However, an intriguing observation emerges when comparing 'X=30' to 'X=20' at high temperatures: 'X=30' exhibits a distinct behavior, dropping lower than 'X=20.' This behavior can be attributed to the significantly higher Fe_2O_3 content in 'X=30,' which may trigger more pronounced endothermic reactions at elevated temperatures, leading to the observed dip in the DSC plot. Furthermore, the different ratios of components in these two systems influence their thermal properties, including heat capacity and heat flow, resulting in distinguishable thermal behavior.

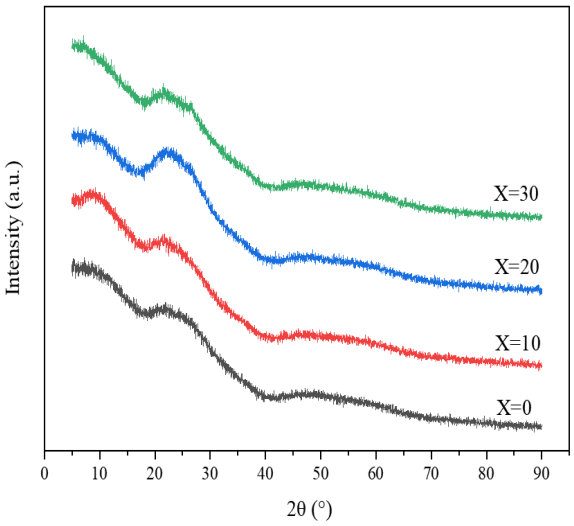

Figure 1. XRD Spectrums of xFe_2O_3-(40-x) K_2O-10MoO_3-50P_2O_5 glasses.

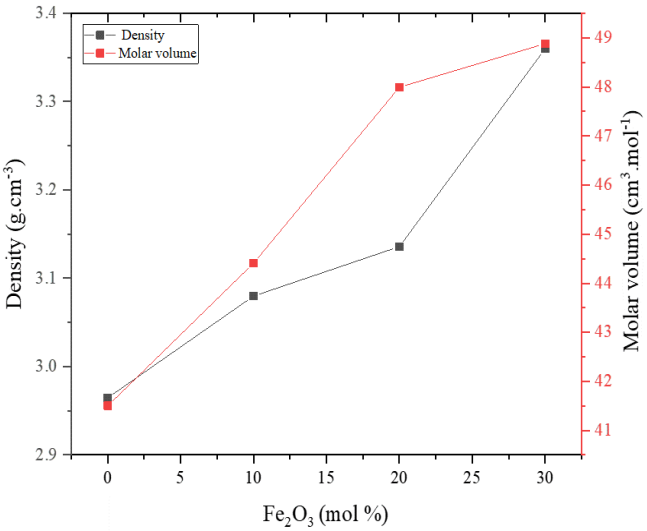

Figure 2. The effect of Fe_2O_3 percentage on density ρ and molar volume V_m in xFe_2O_3- (40-x) K_2O-10MoO_3-50P_2O_5glasses.

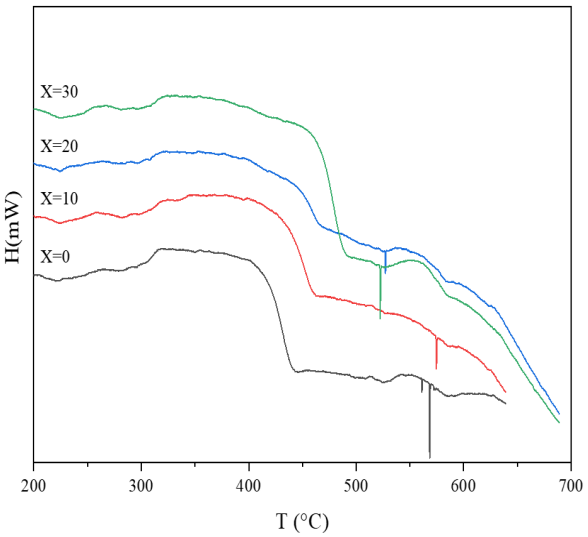

Figure 3. DSC curves of xFe_2O_3-(40-x)K_2O-10MoO_3-50P_2O_5 glasses.

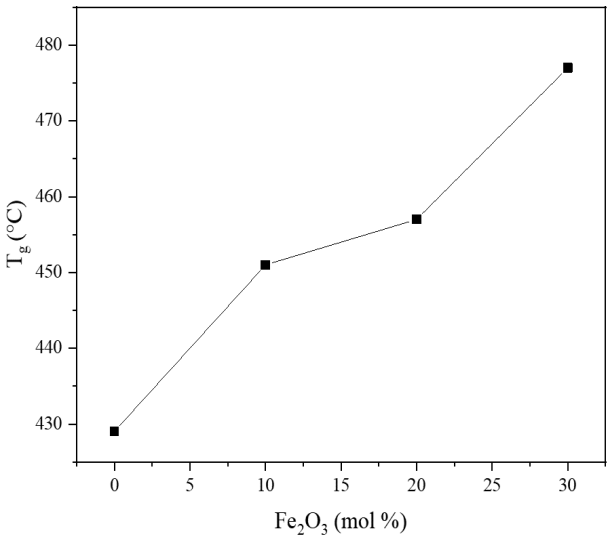

Figure 4. Transition temperature T_g of xFe_2O_3-(40-x)K_2O-10MoO_3-50P_2O_5 glasses as a function of the Fe_2O_3 content.

3.4 Infrared, Raman, and Mössbauer Spectroscopy

Figure 5 depicts the IR bands of our glass system over a frequency range of 400 cm^{-1} to 1400 cm^{-1}. The IR bands were assigned based on prior IR studies on phosphates-based glasses. Practically, all glasses feature eight IR bands at ~1200 cm^{-1}, ~1130 cm^{-1}, ~1080 cm^{-1},~1000 cm^{-1}, ~900 cm^{-1},~850 cm^{-1}, ~750 cm^{-1}, ~650 cm^{-1}, ~540 cm^{-1}, ~500 cm^{-1}.

Bands at ~1200 cm^{-1} and ~1130 cm^{-1} are related to the asymmetric [36] and symmetric [37] stretching vibration of PO_2, respectively.

Two bands at ~1080 cm^{-1} and ~1000 cm^{-1} are ascribed to the asymmetric and symmetric stretching vibration of PO_3, respectively [32].

Two bands ~ 900 cm^{-1} and ~ 850 cm^{-1}, are attributed to asymmetric stretching vibrations of P–O–P linkages [20,36,37] The symmetric stretching vibrations of P–O–P linkages occur at ~750 cm^{-1} [20, 36].

The bands appearing at ~650 cm^{-1}, ~540 cm^{-1} and ~500 cm^{-1} corresponds to the deformation mode of P–O-(PO_4^{3-}) groups [38]. The addition of Fe_2O_3 to the glass composition at x = 0 induces notable spectral changes. With increasing iron oxide concentration, spectral bands experience reduced intensity. A distinct band at around 900 cm^{-1}, associated with asymmetric stretching vibrations of P–O–P linkages, not only diminishes in intensity but also shifts to a higher wavenumber. These shifts signify the disruption of P=O bonds and the formation of P-O-Fe bonds within the glass [39]. The influence of Fe^{3+} ions, known for their smaller ionic size compared to Fe^{2+}, contributes to a narrowing of P-O-P bond angles and a shift of the vibrational band towards higher frequencies [19]. These spectral transformations offer valuable insights into the structural adjustments triggered by the introduction of Fe_2O_3, emphasizing the intricate relationship between chemical composition and vibrational properties within the glass network.

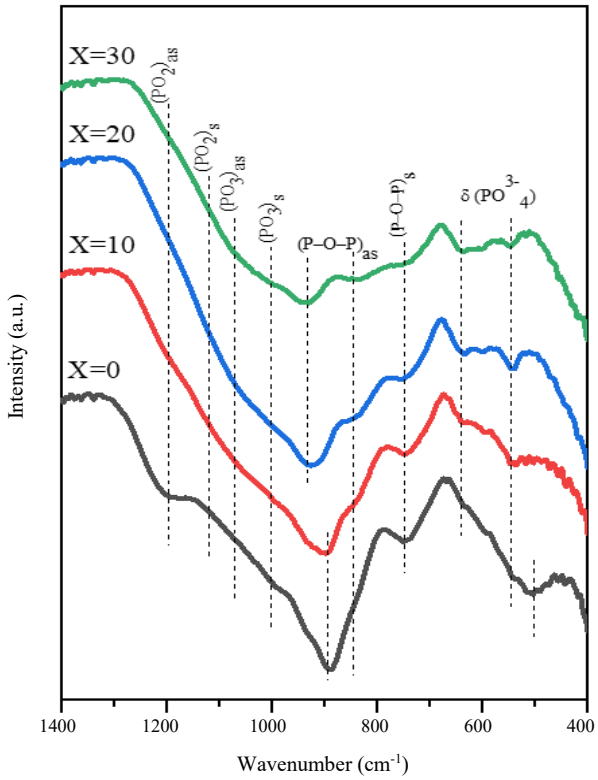

Figure 5. Infrared absorption spectra xFe_2O_3-(40-x) K_2O-10MoO_3-50P_2O_5 glasses.

Table 2. Hyperfine parameters were obtained by adjusting the ^{57}Fe Mössbauer spectra of xFe_2O_3-(40-x)K_2O-10MoO_3-50P_2O_5 glasses.

X	Fe^{3+} (Doublet 1)			Fe^{2+} (Doublet 2)			χ^2
	Area (%)	I.S. ($mm{\cdot}s^{-1}$)	Q.S. ($mm{\cdot}s^{-1}$)	Area (%)	I.S. ($mm{\cdot}s^{-1}$)	Q.S. ($mm{\cdot}s^{-1}$)	
10	99.4	0.40	0.41	0.6	1.04	1.76	0.89
20	97.3	0.37	0.44	2.7	1.17	1.45	1.08
30	96.2	0.34	0.45	3.8	1.14	1.10	1.02

In consistency with Raman spectroscopy, this technique enables the structural characterization of materials by emphasizing the vibrational modes of molecules, serving as a complementary approach to infrared spectroscopy.

The Raman spectra of xFe_2O_3-(40-x) K_2O-10MoO_3-50P_2O_5 glasses were plotted in Figure 6 in a Raman shift range from 100 cm^{-1} to 1100 cm^{-1}. We have assigned the bands according to the literature. All our glass spectra present the same bands characteristic of groups of phosphate with a decrease in their intensity when adding Fe_2O_3. Two bands around ~1060 cm^{-1} and ~ 980 cm^{-1} are associated with the asymmetric and symmetric stretching of PO_3, respectively, suggesting the presence of isolated Q^0 groups [26,28]. The band at ~ 900 cm^{-1} has been linked to asymmetric stretching vibration P-O-P of non-bridging oxygen in PO_4 tetrahedrons in Q^1 groups [28,37]. Both bands at ~830 and ~715 cm^{-1} correspond to the symmetric P-O-P stretching mode ascribed with the bridging oxygen that links two Q^1-tetrahedra or links Q^1 and Q^2 tetrahedra [20,23,26,28,37]. Bands at ~640 cm^{-1} and ~570 cm^{-1} are characteristics of the O-P-O asymmetric bond bending [26,28]. Meanwhile, at ~470 cm^{-1} a band directed to the O-P-O symmetric bond bending [28,37] is detected. The three bands at ~380,~350 and ~295 cm^{-1} are attributed to the deformation mode of P–O^- ($PO4^{3-}$) [23,40,41]. Furthermore, in the wavenumber range of 100 cm^{-1} to 260 cm^{-1}, the Raman bands correspond to the bending of the phosphate bond network and would be difficult to attribute to individual bending vibrations [20,26,28,29,42].

Experimental ^{57}Fe Mössbauer spectroscopy graphs of xFe_2O_3-(40-x)K_2O-10MoO_3-50P_2O_5 glasses are shown in Figure 7, and the calculated hyperfine parameters (relative area, isomer shift "I.S.", quadrupole splitting "Q.S.", fitting uncertainties "χ^2") from the fitting of these spectra are summarized in Table 2. To avoid the addition of Fe_2O_3 in these glasses, the study was limited to iron-rich compositions (x = 10, 20, 30). These three spectra are identical and characteristic of a paramagnetic material. At first sight, we can describe these spectra with a paramagnetic doublet consisting of two very broad lines suggesting the existence of divalent Iron (Fe^{II}) and trivalent Iron (Fe^{III}) within the three glasses.

Even if, in the starting products, the Iron is in the form of Fe_2O_3, the elaborated glasses contain Fe^{2+} ions whose percentages pass from 0.6% for x = 10 to 3.8 % for x = 20. The origin of these ferrous ions is attributed, on the one hand, to the reduction of ferric ions by NH_3 coming from the decomposition of $NH_4H_2PO_4$ and, on the other hand, to the redox equilibrium of Iron in the glass according to the following reaction:

$$2\ Fe^{3+} + O^{2-} \leftrightharpoons 2\ Fe^{2+} + \tfrac{1}{2}\ O_2 \qquad (2)$$

Generally, according to the literature, Fe_2O_3-prepared phosphate melts will mainly decrease to Fe^{2+} [30].

Ferric (Fe^{3+}) sites have a much lower I.S. value than ferrous (Fe^{2+}) sites due to the additional protection of the s-electrons from the nucleus by the extra 3d electron. Fe^{2+} has higher Q.S. values than Fe^{3+} due to its asymmetric $3d^6$ outer shell [43]. Such an increase of χ^2 is related to reducing Fe^{3+} to Fe^{2+}.

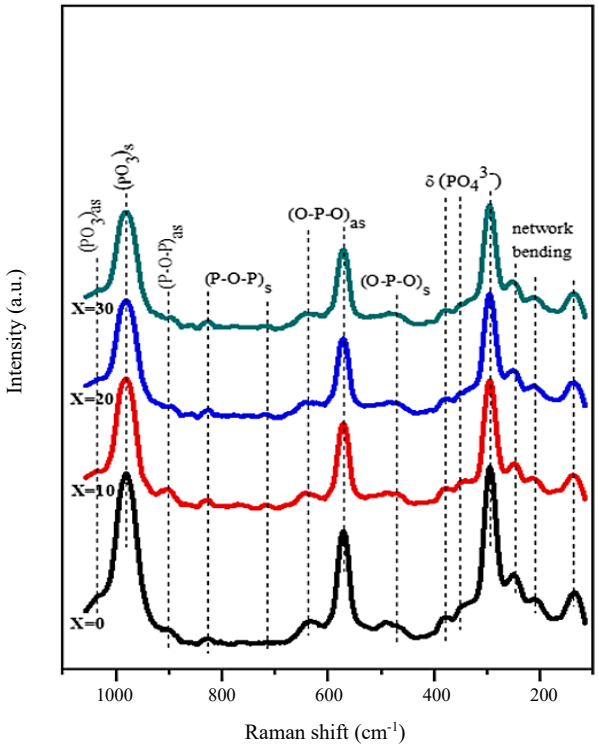

Figure 6. Raman spectra for the xFe_2O_3-(40-x) K_2O-10MoO_3-50P_2O_5 glasses.

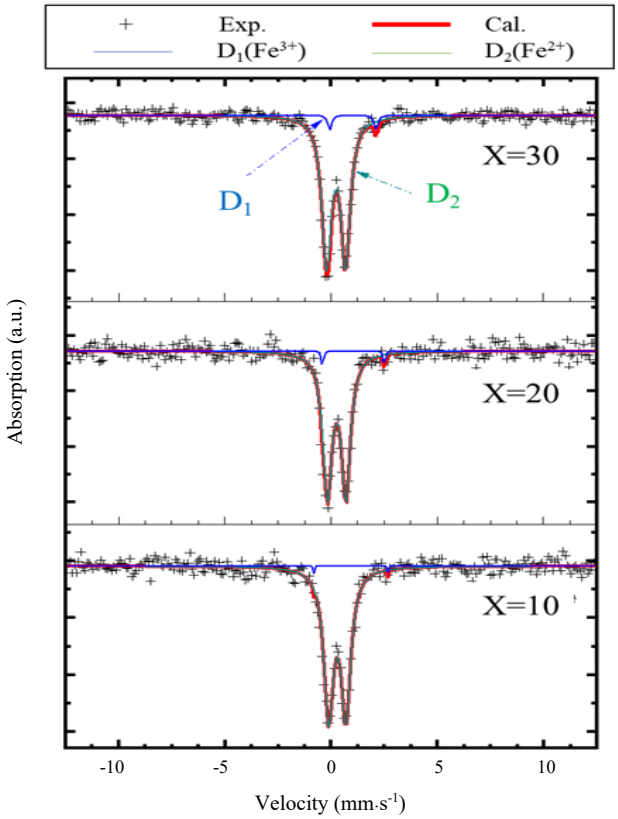

Figure 7. ^{57}Fe Mössbauer spectra collected at 300 K for xFe_2O_3-(40-x) K_2O-10MoO_3-50P_2O_5 glasses. Exp is experimental data, Cal is the calculated spectrum, "D_1" and "D_2" are Doublet 1 and Doublet 2, respectively.

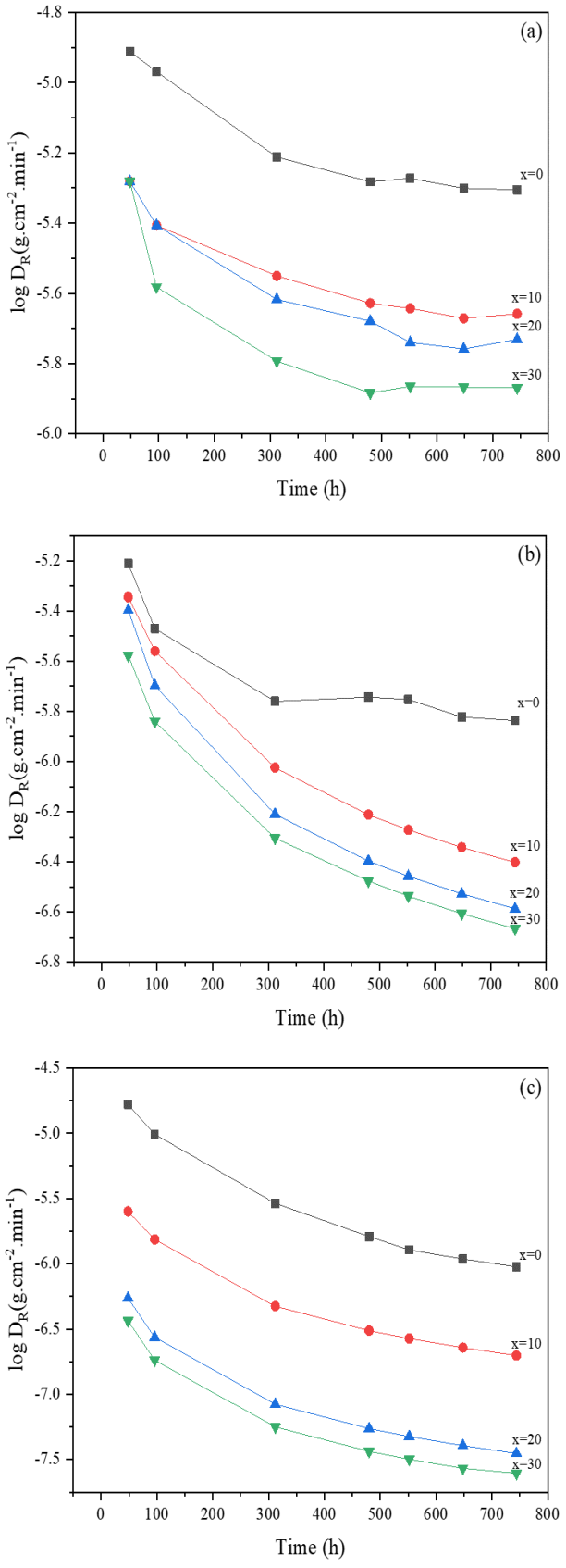

Figure 8. Dissolution rate evolution of xFe_2O_3-(40-x) K_2O-$10MoO_3$-$50P_2O_5$ glasses as a function of Fe_2O_3 content in acidic media HCl (a), deionized water (b), and alkaline media NaOH (c).

3.5 Dissolution rate (D_R)

The dissolution rate is generally determined by the chemical composition, binding strength, bond length, and the number of atoms coordinated in the glassy network [44]. It is important to note that despite the hygroscopicity of pure phosphate glasses, research has shown that adding transition metal oxides (TMOs), namely Fe_2O_3, to the glass matrix enhances the glass's chemical durability.

As shown in Figure 8, a lower DR value in xFe_2O_3-(40-x)K_2O-$10MoO_3$-$50P_2O_5$ glasses pertains to the high Fe_2O_3 concentration, indicating its higher chemical durability. Similar behavior is present for all three mediums. With adding Fe_2O_3, the DR value has decreased significantly. This suggests that the chemical durability increases with increasing Fe_2O_3 concentration, which correlates perfectly with the increase in the glass transition temperature (Figure 4).

The structural source of this gain is the generation of water-resistant Fe-O-P bonds that substitute hydrolyzable P-O-P bonds [45,46] . It should be noted that the chemical durability of the glass will boost with the ionic field strength of cation formers, the P-O-P bond hydrolysis phase, and the quality of metal-oxygen bindings will determine the general solubility [46]. This increases the glass density (ρ) while making the glass structure more compact and improving the aqueous durability as well as the chemical stability of the glasses, as verified by DSC, FTIR, and Raman analysis and justified by Mössbauer spectroscopy.

On the other hand, the comparison of the dissolution rate of $30Fe_2O_3$-$10K_2O$-$10MoO_3$-$50P_2O_5$ glasses in the different media shows an increase from acidic media HCl to alkaline media NaOH through deionized water. The ion exchange process among protons in the solution and the modifying network components could explain the difference in dissolution rate between the three mediums [44].

4. Conclusion

New phosphate glasses containing iron oxide Fe_2O_3 have been synthesized and characterized by X-ray diffraction, DSC, IR, Raman, and Mössbauer spectroscopy. This change in T_g is consistent with the structural modification of the glass proven by IR and Raman spectroscopy. They demonstrate that increasing the Fe_2O_3 content from 0 to 30 mol% promotes depolymerization of the glassy matrix through the creation of dominant short pyrophosphate chains. Once the Fe_2O_3 level hits 30 mol%, this depolymerization becomes more obvious. Its influence on the glassy structure increases, enhancing chemical interconnection by creating Fe-O-P covalent bonds at the expense of readily hydrated P-O-P and K-O-P bonds. Because of the larger ratios of Fe-O-P bonds in the phosphate network, the amorphous material is greatly resistant to chemical attack. From the Mössbauer spectroscopy results, it can be concluded that the increase in Fe_2O_3 content favors a reduction of Fe^{3+} to Fe^{2+} during air melting. Both Fe^{II} and Fe^{III} increase the Fe-O-P covalent band. The generation of short pyrophosphate chains is promoted by incrementing Fe-O-P covalent bonds, strengthening the structure's bonding. We hope that the results of our research will provide theoretical support for the development of phosphate glasses as nuclear waste hosts.

Acknowledgements

We are extremely thankful to the members of the Materials, Nanotechnologies and Environment Laboratory of the Faculty of Science- Mohammed University in Rabat and the Materials Physics Laboratory of FST-Sultan Moulay Slimane University, Beni-Mellal, for this fruitful collaboration

Reference

[1] G. S. Frankel, J. D. Vienna, J. Lian, J. R. Scully, S. Gin, J. V. Ryan, J. Wang, S. H. Kim, W. Windl, and J. Du, "A comparative review of the aqueous corrosion of glasses, crystalline ceramics, and metals," *Npj Materials Degradation*, vol. 2, p. 15, 2018.

[2] Sk. Mahamuda, F. Syed, Ch. B. Annapurna Devi, K. Swapna, M. V. V. K. S. Prasad, M. Venkateswarlu, and A. S. Rao, "Spectral characterization of Dy^{3+} ions doped phosphate glasses for yellow laser applications," *Non-Crystalline Solids*, vol. 555, p. 120538, 2021.

[3] A. Gharbi, S. Ayadi, N. Jouini, F. Schoenstein, H. Oudadess, H. El Feki, and W. Cheikhrouhou-Koubaa, "Original implementation of low-temperature SPS for bioactive glass used as a bone biomaterial," *Mechanical Behavior of Biomedical Materials*, vol. 126, p. 104988, 2022.

[4] D. E. Day, Z. Wu, C. S. Ray, and P. Hrma, "Chemically durable iron phosphate glass wasteforms," *Non-Crystalline Solids*, vol. 241, pp. 1-12, 1998.

[5] A. Faivre, F. Despetis, L. Duffours, and P. Colombel, "Effect of CaO and Al_2O_3 addition on the properties of K_2O–Na_2O–P_2O_5 glass system," *International Journal of Applied Glass Science*, vol. 10, pp. 162-171, 2019.

[6] D. S. Brauer, N. Karpukhina, R. V. Law, and R. G. Hill, "Effect of TiO_2 addition on structure, solubility and crystallisation of phosphate invert glasses for biomedical applications," *Non-Crystalline Solids*, vol. 356, pp. 2626-2633, 2010.

[7] Q. Yin, S. Kang, X. Wang, S. Li, D. He, and L. Hu, "Effect of PbO on the spectral and thermo-optical properties of Nd^{3+} -doped phosphate laser glass," *Optical Materials*, vol. 66, pp. 23-28, 2017.

[8] T. Ishiyama, S. Suzuki, J. Nishii, T. Yamashita, H. Kawazoe, and T. Omata, "Proton conducting tungsten phosphate glass and its application in intermediate temperature fuel cells," *Solid State Ionics*, vol. 262, pp. 856-859, 2014.

[9] B. C. Sales, and L. A. Boatner, "Lead-Iron phosphate glass: A stable storage medium for high-level nuclear waste," *Science*, vol. 226, pp. 45-48, 1984.

[10] S. Kim, K. Han, S. Kim, L. Kadathala, J. Kim, and J. Choi, "Strengthening thermal stability in V_2O_5-ZnO-BaO-B_2O_3-$M(PO_3)_n$ Glass System (M = Al, Mg) for laser sealing applications," *Applied Sciences*, vol. 11, p. 4603, 2021.

[11] N. Kiwsakunkran, W. Chaiphaksa, N. Chanthima, H. J. Kim, S. Kothan, A. Prasatkhetragarn, and J. Kaewkhao, "Fabrication of K_2O–Al_2O_3–Gd_2O_3–P_2O_5 glasses for photonic and scintillation materials applications," *Radiation Physics and Chemistry*, vol. 188, p. 109639, 2021.

[12] H. Takebe, M. Fujisawa, Y. Maeda, and A. Saitoh, "Effect of molybdenum oxide addition on the durability and structure of iron phosphate glasses," *Ceramic Society of Japan*, vol. 129, pp. 105-110, 2021.

[13] S. Punj, J. Singh, and K. Singh, "Ceramic biomaterials: Properties, state of the art and future prospectives," *Ceramics International*, vol. 47, pp. 28059-28074, 2021.

[14] C. José Filho, S. C. Zilio, D. N. Messias, V. Pilla, A. C. A. Silva, N. O. Dantas, and A. A. Andrade, "Effects of aluminum substitution by potassium in the P_2O_5–Al_2O_3–Na_2O–K_2O phosphate glasses," *Alloys and Compounds*, vol. 815, 2020.

[15] A. Moguš-Milanković, A. Šantić, M. Karabulut, and D. E. Day, "Study of electrical properties of MoO_3–Fe_2O_3–P_2O_5 and SrO–Fe_2O_3–P_2O_5 glasses by impedance spectroscopy. II," *Non-Crystalline Solids*, vol. 330, pp. 128-141, 2003.

[16] A. Moguš-Milanković, A. Šantić, A. Gajović, and D. E. Day, "Spectroscopic investigation of MoO_3-Fe_2O_3-P_2O_5 and SrO-Fe_2O_3-P_2O_5 glasses. Part I," *Non-Crystalline Solids*, vol. 325, pp. 76-84, 2003.

[17] I. Ahmed, C. A. Collins, M. P. Lewis, I. Olsen, and J. C. Knowles, "Processing, characterisation and biocompatibility of iron-phosphate glass fibres for tissue engineering," *Biomaterials*, vol. 25, pp. 3223-3232, 2004.

[18] L. Zhang, M. E. Schlesinger, and R. K. Brow, "Phase equilibria in the Fe_2O_3-P_2O_5 system," *American Ceramic Society*, vol. 94, pp. 1605-1610, 2011.

[19] Y. M. Moustafa, K. El-Egili, H. Doweidar, and I. Abbas, "Structure and electric conduction of Fe_2O_3-P_2O_5 glasses," *Physica B Condens Matter*, vol. 353, pp. 82-91, 2004.

[20] X. Li, A. Lu, and H. Yang, "Structure of ZnO-Fe_2O_3-P_2O_5 glasses probed by Raman and IR spectroscopy," *Non-Crystalline Solids*, vol. 389, pp. 21-27, 2014.

[21] A. J. Parsons and C. D. Rudd, "Glass forming region and physical properties in the system P_2O_5-Na_2O-Fe_2O_3," *Non-Crystalline Solids*, vol. 354, pp. 4661-4667, 2008.

[22] P. Bergo, W. M. Pontuschka, and J. M. Prison, "Dielectric properties of P_2O_5-Na_2O-Li_2O glasses containing WO_3, CoO or Fe_2O_3," *Solid State Communications*, vol. 141, pp. 545-547, 2007.

[23] X. Li, Z. Xiao, M. Luo, X. Dong, T. Du, and Y. Wang, "Low melting glasses in ZnO-Fe_2O_3-P_2O_5 system with high chemical durability and thermal stability for sealing or waste immobilization," *Non-Crystalline Solids*, vol. 469, pp. 62-69, 2017.

[24] S. V. Stefanovsky, O. I. Stefanovskaya, S. E. Vinokurov, S. S. Danilov, and B. F. Myasoedov, "Phase composition, structure, and hydrolytic durability of glasses in the Na_2O-Al_2O_3-(Fe_2O_3)-P_2O_5 system at replacement of Al_2O_3 by Fe_2O_3," *Radiochemistry*, vol. 57, pp. 348-355, 2015.

[25] Y. M. Moustafa, and A. El-Adawy, "Structural and physical properties of iron oxychloride phosphate glasses," *Physica Status Solidi (a)*, vol. 179, pp. 83-93,2000.

[26] K. Joseph, T. R. Ravindran, R. Sudha, and R. Asuvathraman, "BaO-Fe_2O_3-P_2O_5 glasses: Understanding the thermal stability," *Nuclear Materials*, vol. 517, pp. 106-112, 2019.

[27] S. T. Reis, M. Karabulut, and D. E. Day, "Chemical durability and structure of zinc–iron phosphate glasses," *Non-Crystalline Solids,* vol. 292, pp. 150-157, 2001.

[28] L. Ma, R. K. Brow, and A. Choudhury, "Structural study of Na_2O-FeO-Fe_2O_3-P_2O_5 glasses by Raman and Mössbauer spectroscopy," *Non-Crystalline Solids*, vol. 402, pp. 64-73, 2014.

[29] S. T. Reis, D. L. A. Faria, J. R. Martinelli, W. M. Pontuschka, D. E. Day, and C. S. M. Partiti, "Structural features of lead iron phosphate glasses," *Non-Crystalline Solids*, vol. 304, pp. 188-194, 2002.

[30] L. Ma, R. K. Brow, L. Ghussn, and M. E. Schlesinger, "Thermal stability of Na_2O-FeO-Fe_2O_3-P_2O_5 glasses," *Non-Crystalline Solids*, vol. 409, pp. 131-138, 2015.

[31] N. Beloued, R. Makhlouk, Y. Er-Rouissi, M. Taibi, M. Sajieddine, S. Aqdim, "Relationship between chemical durability, structure and the ionic-covalent character of Me-O-P bond (Me = Cr, Fe), in the vitreous part of the system $60P_2O_5$-$2Cr_2O_3$-$(38-x)Na_2O$-xFe_2O_3 (with $3 \leq x \leq 33$ mol%)," *Advances in Materials Physics and Chemistry*, vol. 9, pp. 199-209, 2019.

[32] A. Er-Rafai, M. El Moudane, Y. Alaoui, M. Laourayed, M. Taibi, I. Warad, A. Guenbour, A. Bellaouchou, and A. Zarrouk, "Effect of molybdenum oxide on structural characteristics, thermal properties, and chemical dissolution of $(50-x)K_2O$-$xMoO_3$-$50P_2O_5$ phosphate glasses," *Biointerface Research in Applied Chemistry*, vol. 13, p. 294, 2023.

[33] A. Er-Rafai, M. Laourayed, Y. Alaoui, M. El Moudane, N. Lazar, A. Benzaouak, and A. Bellaouchou, "The Effect of Li_2O/K_2O ratio on the electrical and dielectric properties of Li_2O-K_2O-MoO_3-P_2O_5 glasses," *Biointerface Research in Applied Chemistry*, vol. 13, 2023.

[34] M. Jerroudi, L. Bih, M. Azrour, B. Manoun, I. Saadoune, and P. Lazor, "Investigation of novel low melting phosphate glasses inside the Na_2O-K_2O-ZnO-P_2O_5 system," *Inorganic and Organometallic Polymers and Material*, vol. 30, pp. 532-542, 2020.

[35] E. Mohaghegh, A. Nemati, B. Eftekhari Yekta, and S. Banijamali, "Effects of Fe_2O_3 content on ionic conductivity of Li_2O-TiO_2-P_2O_5 glasses and glass-ceramics," *Materials Chemistry and Physics*, vol. 190, pp. 8-16, 2017.

[36] H. Doweidar, Y. M. Moustafa, K. El-Egili, and I. Abbas, "Infrared spectra of Fe_2O_3-PbO-P_2O_5 glasses," *Vibrational Spectroscopy*, vol. 37, pp. 91-96, 2005.

[37] Y. Alaoui, M. Laourayed, A. Er-rafai, M. Hammi, M. El Moudane, M. Boudalia, Z. Sekkat, I. Warad, A. Guenbour, A. Bellaouchou, and A. Zarrouk, "Effect of alumina insertion on structural properties, thermal stability, and chemical durability of potassium calcium based-phosphate glasses," *Inorganic Chemistry Communications*, vol. 142, p. 109632, 2022.

[38] A. Majjane, D. Rair, A. Chahine, M. Et-tabirou, M. Ebn Touhami, and R. Touir, "Preparation and characterization of a new glass system inhibitor for mild steel corrosion in hydrochloric solution," *Corrosion Science*, vol. 60, pp. 98-103, 2012.

[39] J. A. Jiménez, and C. L. Crawford, "Raman and optical spectroscopy study of iron-bearing bio-relevant phosphate glasses: Assessment of γ-ray irradiation effects," *Chemical Physic,* vol. 569, p. 111854, 2023.

[40] N. Guesmia, M. Hamzaoui, L. Beghdadi, M. T. Soltani, and D. de Ligny, "Glass formation, physical and structural investigation studies of the (90-x) Sb_2O_3-$10WO_3$-$xNaPO_3$ glasses," *Materials Today Communications*, vol. 30, p. 103226, 2022.

[41] M. Boudalia, M. Laourayed, M. El Moudane, Z. Sekkat, O. S. Campos, A. Bellaouchou, A. Guenbour, A. J. Garcia, and H. M. A. Amin, "Phosphate glass doped with niobium and bismuth oxides as an eco-friendly corrosion protection matrix of iron steel in HCl medium: Experimental and theoretical insights," *Journal of Alloys and Compounds*, vol. 938, p. 168570, 2023.

[42] A. Šantić, A. Moguš-Milanković, K. Furić, V. Bermanec, C. W. Kim, and D. E. Day, "Structural properties of Cr_2O_3-Fe_2O_3-P_2O_5 glasses, Part I," *Non-Crystalline Solids*, vol. 353, pp. 1070-1077, 2007.

[43] G. L. Williams, "57Fe Mossbauer studies of phosphate-based glass systems," *Sheffield Hallam University, Sheffield*, 1990.

[44] A. Kaaouass, A. Ben Ali, H. Ait Ahsaine, G. Kaichouh, A. Zarrouk, and M. Saadi, "Photocatalytic properties and chemical durability of CaO-B_2O_3-V_2O_5 borovanadate glasses," *Catalysts,* vol. 13, p. 512, 2023.

[45] M. Jerroudi, L. Bih, E. Haily, S. Yousfi, L. Bejjit, M. Haddad, B. Manoun, and P. Lazor, "Optical and electrical properties of manganese doped-alkali metaphosphate glasses," *Materials Today: Proceedings*, vol. 30, pp. 1052-1055, 2020.

[46] F. Muñoz, J. Rocherullé, I. Ahmed, and L. Hu, "Phosphate glasses," in Springer Handbooks, Springer, 2019, pp. 553-594.